Improved Techniques for Relative Radiometric Normalization of High Resolution Satellite Images

Afify, H.,
Department of Public Works, Faculty of Engineering, Tanta University, Tanta, El-Gharbiya, Egypt
E-mail: HafezAfify@yahoo.com

Abstract
Relative radiometric normalization (RRN) is essential for change detection applications. Pseudo Invariant Features (PIF) and Dark and Bright set (DB) are widely used methods to perform RRN. The most important step in these methods is the identification of the normalization targets that should be used to derive the normalization coefficients (gain and offset). This paper first introduces the criteria formula to nominate the normalization targets of typical PIF and DB for QuickBird images. Then, some modifications are suggested to refine the selected normalization targets and to derive the normalization coefficients. The typical and modified PIF and DB methods are applied to normalize two pairs of QuickBird images covering parts of Tanta and Alexandria governorates in Egypt. Finally, the normalized images using the typical and modified PIF and DB methods are examined visually and compared statistically. It was found that the proposed modifications have significantly improved the accuracy of the normalized images.

1. Introduction

Radiometric normalization is a vital preprocessing step required before manipulating multi-temporal remotely sensed images for several mapping applications such as change detection and classification. It aims to minimize the radiometric differences caused by inconsistencies of acquisition conditions rather than changes in surface reflectance. The result of this process is a set of multi-temporal images that appear to have been acquired under the same illumination, atmospheric and sensor geometry conditions. There are two approaches to normalize multi-temporal remotely sensed images; absolute and relative. The absolute radiometric normalization approach utilizes physical models based on the measured atmospheric conditions, solar irradiance, visibility, and humidity at the time of image acquisition (Lo and Yang, 1998). The relative radiometric normalization (RRN) approach utilizes one image as a reference and adjusts the radiometric properties of subject images to match the reference (Yuan and Elvidge, 1996). RRN approach is preferred because no physical data at the time of satellite overpasses is required. Many publications reviewed RRN methods, for example (Elvidge et al., 1995, Yang and Lo, 2000, Heo and Fitzhugh, 2000, Du et al., 2002, Canty et al., 2004, Darren et al., 2006, Hong and Zhang, 2007 and Canty and Nielsen, 2008). However, the methods of RRN approach are classified into three groups; statistical adjustments, histogram matching and linear regression.

Linear regression normalization methods are based on the fundamental premise that the radiance reaching the satellite sensor in a given band can be expressed as a linear function of reflectivity (Schott et al., 1988). The digital numbers are also a simple linear function of the radiance reaching the sensor. Thus, the atmospheric and calibration differences between scenes are linearly related (Hall et al., 1991). Accordingly the RRN can be performed using a linear equation:

$$Y_i = a_i X_i + b_i$$

Equation 1

X_i and Y_i = the DN of band (i) for subject image X and reference image Y.

a_i and b_i = the normalization coefficients (gain and offset)

Simple regression (SR), pseudo invariant features (PIF), and dark and bright set (DB) are three linear regression methods widely used to perform RRN. The primary difference between these methods is the procedure of selecting the normalization targets that have no real surface change and therefore employed to derive the normalization coefficients. In SR method all the pixels of the image are used in a least-squares regression to derive the normalization coefficients as follows:

$$a_i = V_{(X_i Y_i)} / V_{(X_i X_i)}$$

Equation 2

$$b_i = \overline{Y}_i - a_i \overline{X}_i$$

Equation 3

$\overline{X}_i$ and $\overline{Y}_i$ = the means of band (i) for subject image X and reference image Y.

$V_{(X_i Y_i)}$ = the covariance of band (i) between subject and reference images.

$V_{(X_i X_i)}$ = the variance of band (i) for the subject image.

In PIF and DB methods a subset of pixels is automatically selected as normalization targets using a criteria formula for each sensor according to the spatial, spectral, and radiometric properties of the acquired images. In this research the PIF and DB criteria formula used with QuickBird multi-temporal images to select the normalization targets is introduced. Then, a suggested procedure to refine these selected normalization targets is described and applied to normalize two pairs of QuickBird images covering parts of Tanta and Alexandria governorates in Egypt. The normalized images using typical and modified PIF and DB methods are examined visually and compared statistically to those obtained using the SR method. The processing steps of this study were performed by the aid of PCI digital image processing software version 10.3 from Geomatica, Ottawa, Canada.

2. Study Site and Data Sets

Two pairs of QuickBird images were used. Figure 1 shows the two images of the first pair. They were acquired in 2003, and 2010, covering Tanta campus and adjacent areas, Egypt. Image 2003 was registered to image 2010. The two images of the second pair were acquired in 2002, and 2007, covering a part of the northern coast of Alexandria along the Mediterranean Sea, Egypt as shown in Figure 2. Image 2002 was tied down to image 2007. The images of the two pairs are cloud free with a size of 600 pixels by 500 pixels, 2.4 m each but more buildings shadow can be observed in Alexandria image pair.

The second order polynomial and the nearest neighbor resampling technique were applied to perform the registration process. The root mean square errors of the registration process are less than half a pixel for both pairs.

3. Methods

3.1 Typical Pseudo Invariant Features (PIF) Method

This method was developed by Schott et al., (1988). PIF are objects with nearly invariant reflectivity between two acquisition dates. They are man-made objects whose reflectance is independent of seasonal or biological cycles such as concrete, asphalt roads, and rooftops. Regarding the previous literature (Elvidge et al., 1995, Yuan and Elvidge, 1996 and Yang and Lo, 2000), the criteria formula used with Landsat to select the PIF set cannot be used with QuickBird because of the drastic differences in spatial, spectral, and radiometric characteristics between Landsat and QuickBird images. Therefore, for QuickBird images the PIF set is defined based on the intersection of the infrared to red ratio threshold mask with the infrared threshold mask as follows:

$$\text{PIF set} = \left(\frac{\text{band 4}}{\text{band 3}} < 1.1 \text{ and, band } 4 > 400 \right)$$

Equation 4

The threshold values of equation (4) are determined by interactive observation of different threshold results. Once the PIF are selected in the subject and reference images, the normalization coefficients was derived as follows:

$$a_i = \sigma Y_i / \sigma X_i$$

Equation 5

$$b_i = \overline{Y}_i - a_i \overline{X}_i$$

Equation 6

σX_i and σY_i = the standard deviation of the PIF set for band (i) in subject image X and reference image Y.

$\overline{X}_i$ and $\overline{Y}_i$ = the means of band (i) for subject image X and reference image Y.

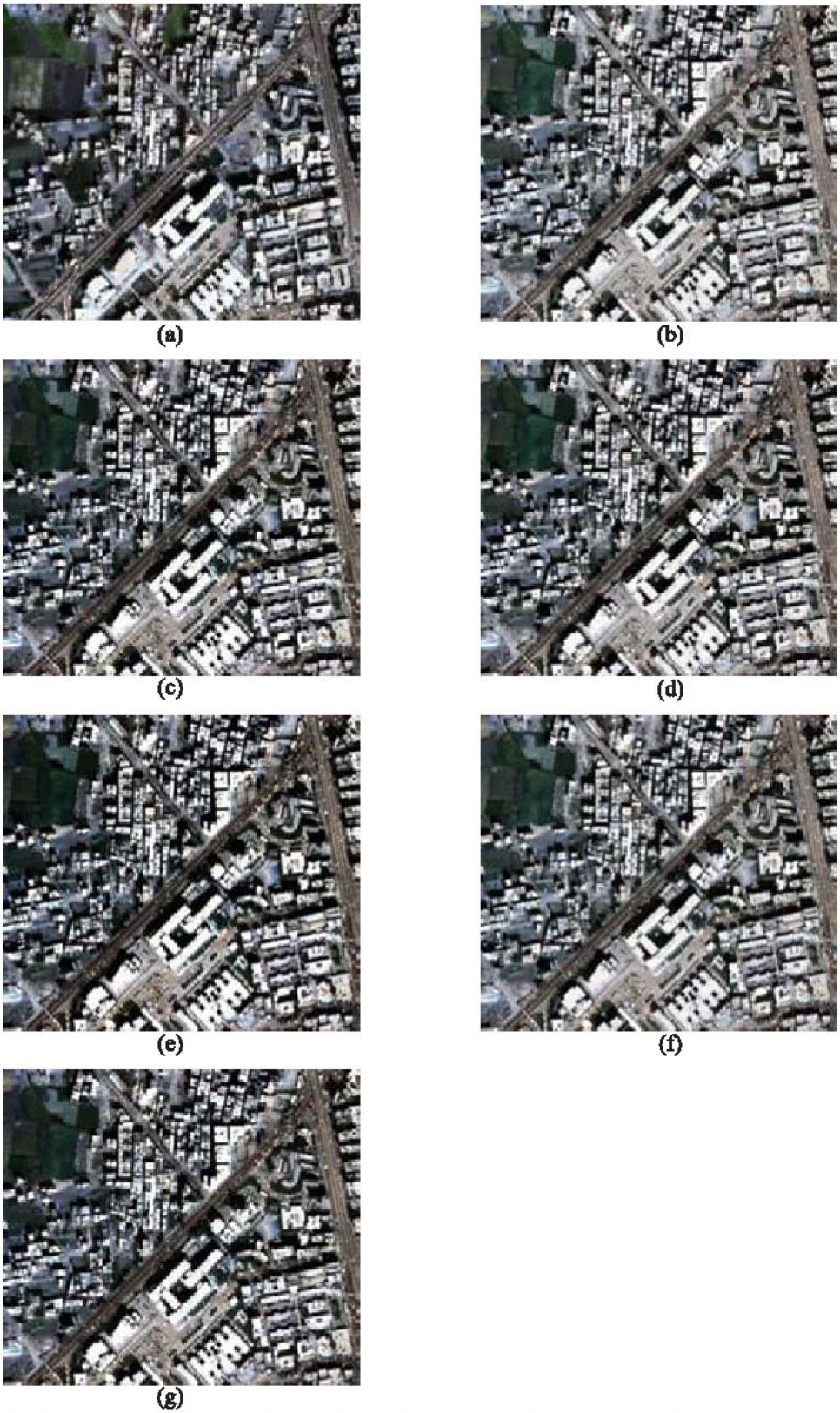

Figure 1: A subscene of the reference image, the subject image and the normalized images for Tanta site. (a) The reference image, (b) The subject image, (c) SR normalized image, (d) PIF normalized image (e) PIF-mod normalized image, (f) DB normalized image, (g) DB-mod normalized image

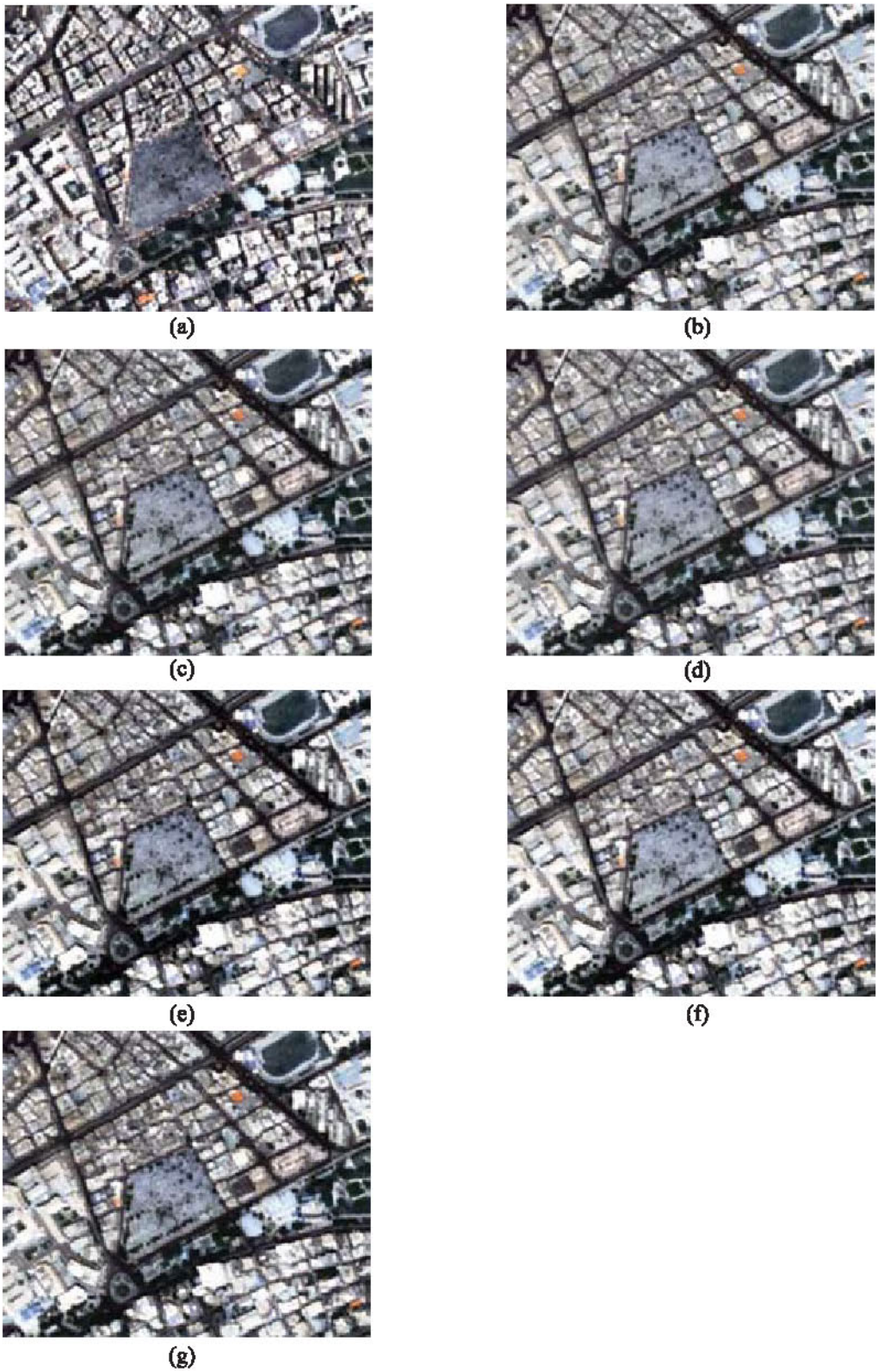

Figure 2: A subscene of the reference image, the subject image and the normalized images for Alexandria site (a) The reference image, (b) The subject image, (c) SR normalized image, (d) PIF normalized image (e) PIF-mod normalized image, (f) DB normalized image, (g) DB-mod normalized image

3.2. Modified PIF (PIF-mod) Method

The suggested modifications of PIF method involved the procedure of selecting the PIF set and the equations of deriving the normalization coefficients as well. The application of PIF-mod method for each QuickBird pair was performed according to the following processing steps:

- The subject image was geometrically registered to the master image.
- PIF sets were independently determined in the subject and reference images according to equation (4).
- A refinement procedure for the selected PIF sets was applied to determine the refined PIF-mod set as the intersection of the individual PIF masks in subject and reference images using logical "AND".
- The refined PIF-mod set was utilized to derive the normalization coefficients by least-squares regression according to equations (2 and 3) and not like typical PIF method where equations (5 and 6) were used to derive the normalization coefficients.

3.3. Dark and Bright (DB) Method

Hall et al., (1991) used the average of a set of dark and bright (DB) pixels to determine the normalization coefficients. The DB set is extracted from the subject and reference images using Kauth-Thomas (KT) greenness - brightness transformation. Yarbrough et al. (2005) developed the transformation formula to be used only with QuickBird images. In some satellites where there are only three bands other Kauth-Thomas (KT) greenness - brightness transformation equations with different coefficients are required. However the transformation equations for QuickBird images are as follow:

Brightness = 0.319 (band1) + 0.542 (band2) + 0.490 (band3) + 0.604 (band4).

Greenness = -0.121 (band1) – 0.331 (band2) – 0.517 (band3) + 0.780 (band4)

The dark set and bright set were defined using the greenness and brightness bands according to the criteria formula:

$$\text{Dark set} = (\text{greenness} \le 1 \text{ and, brightness} \le 460)$$

Equation 7

$$\text{Bright set} = (\text{greenness} \le 1 \text{ and, brightness} \ge 950)$$

Equation 8

The threshold values of dark and bright sets were determined by interactive observations of different threshold results. The normalization coefficients were obtained based only on the determined DB sets in both the subject and reference images according to:

$$a_i = (\bar{Y}_i^b - \bar{Y}_i^d) / (\bar{X}_i^b - \bar{X}_i^d)$$

Equation 9

$$b_i = \bar{Y}_i^d - a_i \bar{X}_i^d$$

Equation 10

$\bar{Y}_i^b$ and $\bar{Y}_i^d$ = the means of the bright set (b) and the dark set (d) of band (i) in reference image Y.

$\bar{X}_i^b$ and $\bar{X}_i^d$ = the means of the bright set (b) and the dark set (d) of band (i) in subject image X.

3.4. Modified DB (DB-mod) method

The application of DB-mod method was performed according to the following processing steps:

- The subject image was geometrically registered to the master image.
- The normalization targets (dark and bright sets) were independently determined in subject and reference images according to equations (7 and 8).
- The refined dark set was determined as the intersection of the two dark masks in subject and reference images using logical "AND".
- The refined bright set was also identified as the intersection between the two bright masks in subject and reference images using logical "AND".
- The refined DB-mod set was determined by grouping together the refined dark set and refined bright set using logical "OR".
- The normalization coefficients were derived based on the refined DB-mod set by least-squares regression according to equations (2 and 3) and not like typical DB method where equations (9 and 10) were used to derive the normalization coefficients.

4. Results and Analysis

Typical and modified PIF and DB methods were applied to normalize the two pairs of QuickBird images. For the comparison purpose SR method was also applied since many previous works demonstrated that it provides the best results. The calculated normalization coefficients (gain and offset) of each method are given for Tanta pair and Alexandria pair in tables (1 and 2) respectively. The gain and offset of each method were utilized to normalize the subject image of each pair according to equation (1). A subscene of the reference, subject, and normalized images of the two datasets are shown in figures (1 and 2). The visual inspection of Tanta images revealed that all the normalized images are radiometrically more similar to the reference image than the subject image. In addition, the normalized images using SR, PIF-mod and DB-mod methods have closer appearance to the reference image than those obtained using the typical PIF and DB methods. As for Alexandria images, the same visual appearance results can be drawn. However, the visual inspection is prone of subjectivity, and a quantitative evaluation is essential. Therefore, the root mean square error (RMSE) is used to statistically compare the normalized images to the reference image of each data set.

$$RMSE_i = \sqrt{\frac{1}{n} \sum_{i=1}^{n} (Y_i - X'_i)^2}$$

n = the total number of pixels in the scene

Y_i = the digital number of band (i) of the reference image.

X'_i = the digital number of band (i) of the normalized image.

The RMSEs of the normalized images and the numbers of pixels used to derive the normalization coefficients by different normalization methods are listed in tables (3 and 4) for Tanta and Alexandria pairs respectively. The RMSE of the raw subject image is also provided. Figure 3 shows the graphical representation of the average RMSEs of different normalization methods. From tables (3) and (4), it can be noted that for the two pairs, the normalized images using all the applied methods have provided RMSEs that are less than the RMSEs of the subject image. This means that the normalized images are radiometrically more similar to their reference image. The applied methods can be ranked in descending order according to their average RMSEs for Tanta pair as SR, PIF-mod, DB-mod, PIF, and DB while for Alexandria pair as SR, DB-mod, PIF-mod, DB, and PIF. The RMSEs of DB-mod and PIF-mod methods are very close to that of SR method. This confirms the visual inspection results for the normalized images using these three methods. It can be also noted that for both Tanta and Alexandria image pairs, the obtained RMSEs due to applying PIF-mod and DB-mod methods are smaller than those obtained using typical PIF and DB methods. This proved that the proposed modifications applied in PIF-mod and DB-mod methods to refine the normalization targets and to derive the normalization coefficients are efficient since they improved the radiometric closeness of the normalized images to their reference image.

Table 1: The normalization coefficients for Tanta image pair

Method	Band 1		Band 2		Band 3		Band 4	
	(a)	(b)	(a)	(b)	(a)	(b)	(a)	(b)
SR	0.38	171.89	0.42	230.88	0.46	151.29	0.49	145.37
PIF	0.68	93.31	0.72	117.67	0.77	67.72	0.82	41.49
PIF-mod	0.24	259.64	0.27	399.24	0.30	303.68	0.31	316.15
DB	0.79	63.03	0.82	76.72	0.87	39.06	0.93	8.50
DB-mod	0.59	125.79	0.60	191.88	0.62	142.16	0.63	143.24

Table 2: The normalization coefficients for Alexandria image pair

Method	Band 1		Band 2		Band 3		Band 4	
	(a)	(b)	(a)	(b)	(a)	(b)	(a)	(b)
SR	0.48	181.20	0.49	272.06	0.54	182.19	0.60	174.15
PIF	0.89	68.00	0.90	147.44	0.92	123.49	0.89	79.69
PIF-mod	0.37	283.54	0.39	449.57	0.40	349.33	0.40	360.98
DB	0.78	75.93	0.82	103.78	0.85	65.83	0.85	74.06
DB-mod	0.60	165.74	0.63	250.96	0.69	167.13	0.71	161.79

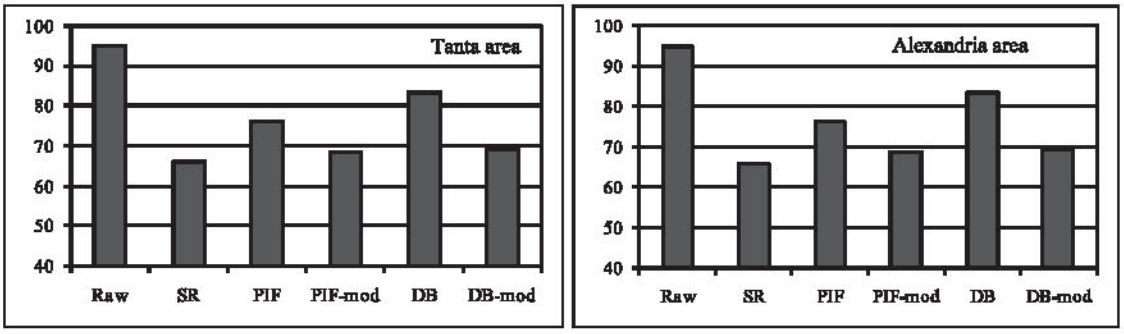

Figure 3: Average RMSEs of different normalization methods for Tanta and Alexandria image pairs

Table 3: The number of normalization pixels and RMSEs of different normalization methods for Tanta image pair

Method	Reference (2010)		Subject (2003)		Root mean square error				
	Number	%	Number	%	Band 1	Band 2	Band 3	Band 4	Average
Raw	300000	100	300000	100	53.90	110.41	102.97	112.61	94.97
SR	300000	100	300000	100	33.59	72.44	72.27	85.39	65.92
PIF	52304	17.4	77851	26.0	39.28	84.43	83.72	97.83	76.32
PIF-mod	36199	12.1	36199	12.1	34.95	75.38	75.35	88.97	68.66
DB (D) (B)	44096 (22873) (21223)	14.7	93232 (36337) (56895)	31.1	43.72	92.58	91.37	106.20	83.47
DB-mod (D) (B)	31232 (15229) (16003)	10.4	31232 (15229) (16003)	10.4	36.54	76.82	75.51	87.93	69.20

Table 4: The number of normalization pixels and RMSEs of different normalization methods for Alexandria image pair

Method	Reference (2007)		Subject (2002)		Root mean square error				
	Number	%	Number	%	Band 1	Band 2	Band 3	Band 4	Average
Raw	300000	100	300000	100	101.86	201.52	184.96	189.05	169.35
SR	300000	100	300000	100	83.30	168.90	157.84	165.09	143.78
PIF	114756	38.3	141867	47.3	95.30	190.64	176.88	178.06	160.22
PIF-mod	89976	30.0	89976	30.0	84.17	170.44	160.34	171.51	146.62
DB (D) (B)	146219 (15794) (130425)	48.7	186680 (22649) (164031)	62.2	89.74	183.04	170.73	174.66	154.54
DB-mod (D) (B)	120439 (14199) (106240)	40.2	120439 (14199) (106240)	40.2	84.43	171.45	161.07	167.00	145.99

This can be interpreted as the intersection of the individual normalization targets masks in subject and reference images excluded the pixels of shadow or relief displacement at different directions of the features due to different sensor-object-illumination geometry from the selection as normalization targets. It also excluded the pixels of poor registration along the boundaries of different features. For each of the two data sets, the number of normalization pixels used for PIF-mod and DB-mod methods are much smaller than those for PIF and DB method even though the modified methods have provided higher accuracy (smaller RMSEs) compared to the traditional ones. This confirms the

capability of the used refinement procedure to select normalization targets that provide a comprehensive representation of non-surface radiometric differences between different acquisition dates. For all normalization methods the improvement percentage in Alexandria pair is less than that of Tanta pair. As example, for SR method the average RMSE was improved from 169.35 to 143.78 (15.1%) for Alexandria pair, and from 94.97 to 65.92 (30.59%) for Tanta pair. This is because the nature of the images and the features distribution in the study area. As for Alexandria images, the dense and high buildings with their attributed shadows and relief displacement at different directions due to different illumination and viewing angles degraded the improvement percentage.

5. Conclusion

This study introduces the criteria formula required to select the normalization targets of typical PIF and DB methods for QuickBird images. A new procedure is suggested to refine these selected normalization targets and to derive the normalization coefficients resulting in the modified PIF and DB methods. The performance of typical and modified PIF and DB normalization methods is examined to normalize two multi-temporal QuickBird images. All the applied methods have shown improvement of the radiometric similarity between the subject image and the reference image. The PIF-mod and DB-mod methods have improved the accuracy and produced very close normalized images comparable to that obtained using SR method. It is expected that these two modified methods produce higher accuracy than SR method especially if the images contain large areas of change or clouds. As the SR method uses all the pixels equally, there is a possibility to include areas of actual changes and clouds in normalization equations. The typical PIF and DB methods have provided the least accuracy. The PIF-mod and DB-mod methods have produced normalized images with higher accuracy (less RMSEs) than those obtained using the typical PIF and DB methods, though the number of normalization pixels used for PIF-mod and DB-mod methods are less than that used for PIF and DB methods. This proved the effectiveness of the suggested refinement procedure to determine less number of normalization targets having more representation of the radiometric differences caused by inconsistencies of acquisition conditions rather than changes in surface reflectance. The performance of RRN methods is dependent on the nature of the images, land-cover classes and distribution, and the similarity of illumination and viewing angles between the reference and subject images.

References

Canty, M. J., and Nielsen, A. A., 2008, Automatic Radiometric Normalization of Multitemporal Satellite Imagery with the Iteratively Re-Weighted MAD Transformation. *Remote Sensing of Environment*, 112, 1025–1036.

Canty, M. J., Nielsen, A. A., and Schmidt, M., 2004, Automatic Radiometric Normalization of Multitemporal Satellite Imagery. *Remote Sensing of Environment*, 91(3–4), 441–451.

Darren T. J., Arthur L. F., and Roger D. W., 2006, Radiometric Correction Techniques and Accuracy Assessment for Landsat TM Data in Remote Forested Regions. *Canadian Journal of Remote Sensing*, 32(5), 330–340

Du, Y., Teillet, P. M., and Cihlar, J., 2002, Radiometric Normalization of Multitemporal High-Resolution Satellite Images with Quality Control for Land Cover Change Detection. *Remote Sensing of Environment*, 82(2), 123–134.

Elvidge, C. D., Yuan, D., Werackoon, R. D., and Lunetta, R. S., 1995, Relative Radiometric Normalization of Landsat Multispectral Scanner (MSS) Data using an Automated Scattergram Controlled Regression. *Photogrammetric Engineering and Remote Sensing*, 61(10), 1255-1260.

Hall, F. G., Strebel, D. E., Nickeson, J. E., and Goetz, S. J., 1991, Radiometric Rectification: Toward a Common Radiometric Response among Multi-Data, Multi-Sensor Images. *Remote Sensing of Environment,* 35(1), 11– 27.

Heo, J., and Fitzhugh, T. W., 2000, A Standardized Radiometric Normalization Method for Change Detection using Remotely Sensed Imagery. *Photogrammetric Engineering and Remote Sensing,* 66(2), 173-181.

Hong G., and Zhang, Y., 2007, A Comparative Study On Radiometric Normalization using High Resolution Satellite Images. *International Journal of Remote Sensing*, 29(2), 425-438.

Lo, C. P., and Yang, X., 1998, Some Practical Considerations of Relative Radiometric Normalization of Multidate Landsat MSS Data for Land Use Change Detection. *Proceedings of ASPRS/RTI 1998 Annual Convention*, Tampa, Florida, 1184-1193.

Schott, J. R., Salvaggio, C., and Volchok, W. J., 1988, Radiometric Scene Normalization using Pseudoinvariant Features. *Remote Sensing of Environment*, 26(1), 1-16.

Yang, X., and Lo, C. P., 2000, Relative Radiometric Normalization Performance for Change Detection from Multidate Satellite Images. *Photogrammetric Engineering & Remote Sensing*, 66(8), 967-980.

Yarbrough, L. D., Easson, G., and Kuszmaul, J. S., 2005, QuickBird 2 Tasseled Cap Transform Coefficients: A Comparison of Derivation Methods. *Proceeding of ASPRS Conference Pecora 16, October 23-27, 2005, Sioux Falls, South Dakota.*

Yuan, D., and Elvidge, C. D., 1996, Comparison of Relative Radiometric Normalization Techniques. *ISPRS Journal of Photogrammetry and Remote Sensing*, 51(3), 117-126.